LA-7701-PR

Progress Report

Superconducting Magnetic Energy Storage (SMES) Program

January 1—December 31, 1978

University of California

LOS ALAMOS SCIENTIFIC LABORATORY

Post Office Box 1663 Los Alamos, New Mexico 87545

LA-7701-PR
Progress Report
UC-20b and UC-94b
Issued: February 1979

Superconducting Magnetic Energy Storage (SMES) Program

January 1—December 31, 1978

Compiled by
John D. Rogers

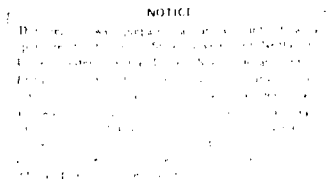

SUPERCONDUCTING MAGNETIC ENERGY STORAGE (SMES) PROGRAM

January 1 – December 31, 1978

Compiled by

John D. Rogers

ABSTRACT

Work is reported on the development of two superconducting magnetic energy storage units. One is a 30-MJ unit for use by the Bonneville Power Administration to stabilize power oscillations on their Pacific AC Intertie, and the second is a 1- to 10-GWh unit for use as a diurnal load-leveling device. Emphasis has been placed on the stabilizing system. The engineering specification design of the 30-MJ superconducting coil was completed and a contract will be placed for the coil fabrication design. Bids have been received for the stabilizing system 10-MW converter and coil protective dump resistor. These components will be purchased in 1979. The reference design for the 1- to 10-GWh diurnal load-leveling unit has been totally revised and is being assembled in redrafted report form. Plans are to build a 10- to 30-MWh prototype diurnal load-leveling demonstration unit.

I. SUMMARY

The goal of the Los Alamos Scientific Laboratory's (LASL's) superconducting magnetic energy storage (SMES) program is to develop electrical units to store energy in a magnetic field around a coil or inductor. The magnetic field is created by an electrical current flowing in a conductor that is in a superconducting state. Many materials, such as niobium-titanium, lose their resistance to electrical currents, that is, become superconducting, at low temperatures. Electrical utilities can use 1- to 10-GWh SMES units to meet

diurnal variations in consumer power demand. During the night, when consumption is low, generators can supply energy to the unit. During the day, when demand is high, energy can be drawn from the SMES unit. In another application, smaller 30-MJ (8.3-kWh) SMES units can be used to damp out the short-term power oscillations in complex electrical grids that sometimes limit maximum power transmission.

This report describes the progress made in the design of the 30-MJ stabilizing SMES unit and testing of superconductor for the unit. A decision was made to make a point reference design of a 1-GWh diurnal load-leveling SMES unit as a system for which a larger market will exist for utility application. Extrapolation to a 10-GWh unit is straightforward. The components that must be considered for both systems are the superconductor itself; the coil; the dewar, which will contain the coil and liquid helium to cool it to a superconducting state; the cryogenic equipment to make liquid helium and keep it cold; the electrical equipment to connect the coil to the power grid; and finally, the monitor and control equipment to regulate the safe operation of charge and discharge of the coil.

The following have been accomplished this year. The design parameters for the stabilizing unit were revised. These are given in Tables I, II, III, and IV. The engineering specification design for the 30-MJ superconducting coil was completed, and bids for the industrial fabrication of the coil have been obtained. The engineering design of the 10-MW converter was completed and bids for its fabrication have also been received. Samples of the first- and second-level superconducting cables for the 30-MJ coil have been tested for both limiting transport current and cryogenic stability. Long lengths of complete 5-kA superconducting prototype cable for the 30-MJ coil have been ordered. The superconducting wire for the coil and the SCRs with their heat sinks for the converter have been purchased.

Work on the 1-GWh load-leveling SMES reference design was expanded this last year to use outside engineering and industrial firms to conduct studies in several specific areas to establish more reliable costs. Major areas evaluated in this manner were the methods and costs for excavating for locating the system underground and for obtaining high-purity aluminum for the superconductor matrix material. In addition, a cost optimization study was performed for 1- and 5-GWh, constant-power converters. Extensive design exploration was committed to the dewar with both thermal and mechanical stresses

considered. A conductor design, not investigated in detail heretofore, has been studied as a useful alternative. The conductor provides for a multiple-layer coil operated at 50 kA with the Lorentz forces being taken as radial and axial loads on the dewar. Supporting testing and development work for both systems are reported.

II. BONNEVILLE POWER ADMINISTRATION STABILIZING SMES UNIT

A. Introduction

The electric utility systems of the Pacific Northwest and southern California are connected primarily by the 500-kV Pacific AC Intertie and the ±400-kV Pacific HVDC Intertie, which has a thermal rating of 1440 MW. At present, the series capacitors impose a thermal limit of 2800 MW on the AC Intertie. Two large generating systems joined by a relatively weak link such as the AC Intertie are likely to have stability problems; and, in fact, since energization of the AC Intertie in 1968, negatively damped power oscillations as large as 300 MW peak to peak have occurred, especially under heavy loading. These instabilities, which have a dominant frequency of 0.35 Hz, make it impossible to use the AC Intertie to its design capacity. With the installation of power system stabilizers on most of the generators in the system, the allowable power transfer on the AC Intertie increased to 2100 MW. The power transfer capability of the AC Intertie was further improved when the Bonneville Power Administration (BPA) implemented a control system to modulate ±40 MW of the power flow at the northern terminal of the HVDC Intertie. However, a dc power modulation of only 5 MW peak to peak damps oscillations on the parallel ac line; and the AC Intertie can now carry up to 2500 MW without experiencing instability.

It appears that a small SMES system could also serve this purpose. Such a unit, when located close to the center of power generation in the Pacific Northwest, would act as an alternate source of damping for the HVDC Intertie modulation system. The first iteration on a detailed design was reported upon in LA-7312-P (June 1978), and the same parameters appeared in LA-7294-PR. A second iteration, in which the structural details were more carefully considered, led to a revised set of parameters given below. A testing program has

been under way in several areas. Components for the system have been acquired and contracts for other components are being negotiated.

B. Superconductor and Coil Design (J. C. Bronson, R. I. Schermer; W. E. Dunwoody, Q-13; B. P. Turck, Saclay)

The coil structural concept, which is based on the superconducting coil fabricated for the LASL Magnetic Energy Transfer and Storage (METS) program by Westinghouse, utilizes G-10 shells between the layers of conductor. The resulting structure promises to be mechanically stable with stress cycling and to yield close dimensional tolerances during fabrication. Detailed design requires extra material such that the overall current density is reduced from that considered previously. This leads to a larger coil, which operates at a lower magnetic field. Table I gives a revised set of operating parameters. The conductor consists of ten subcables rather than twelve, but the conductor length and the required component masses are very close to those previously reported. Table II gives the revised coil parameters, Table III gives the revised conductor parameters, and Table IV gives a conservative estimate for the expected electromagnetic losses in the coil using these new dimensions.

The conductor will consist of ten individually cryostable sub-bundles, cabled about a steel support strap. The main coil support elements will be a thick, filament-wound, fiber-reinforced plastic (FRP) inner mandrel and vertically placed G-10 CR strips that define vertical cooling channels and provide

TABLE I

REVISED 30-MJ OPERATING PARAMETERS

Energy stored at full charge	30 MJ
Energy stored at end of discharge	20.9 MJ
Current at full charge	4900 A
Maximum field at full charge	2.8 T
Inductance	2.5 H
Operating temperature	4.5 K
Mean radius	1.53 m
Height	1.15 m
Radial thickness	42 cm
Number of turns	900

TABLE II

PARAMETERS OF A 30-MJ SYSTEM STABILIZING COIL

Energy stored at full charge	30 MJ
Energy stored at end of discharge	20.9 MJ
Current at full charge	4.9 kA
Insulation standoff voltage	10 kV
Maximum field at full charge	2.8 T
Inductance	2.5 H
Operating temperature	4.5 K
Mean radius	1.53 m
Height	1.15 m
Radial thickness	0.40 m
Number of turns	900
Winding pattern	layer
Number of layers	20
Number of turns per layer	45
Coolant channels axial and radial	2 mm
Conductor length	8652 m
NbTi volume	2.34×10^{-2} m^3
NbTi mass	131 kg
Composite core mass	756 kg
First subcable mass	5750 kg
Second subcable mass	6750 kg
Strap mass	3850 kg
Current density in copper at 4.9 kA	6.7×10^7 A/m^2
Current density in superconductor	1.8×10^9 A/m^2

horizontal slots in which the conductor will be wound. A combination of winding tension and the greater thermal contraction of steel than FRP will result in a tensile preload of approximately 140 MPa (20 ksi) in the steel strap. The major result of this design concept is that the plastic structure will experience only a very small portion of the cyclic stress while the tension in the steel strap ranges approximately between 280 MPa (40 ksi) and 235 MPa (34 ksi) during the operating cycle. This combination of average stress and

TABLE III

SPECIFICATIONS FOR A CRYOSTABLE CONDUCTOR FOR A 30-MJ SYSTEM STABILIZING COIL

A.	Superconductor Composite Core	
	Area of NbTi	4.85×10^{-2} mm^2
	Filament diameter	6.5 μm
	Number of filaments	1464
	Strand diameter, D_S	0.462 mm
	Cu to NbTi ratio	2.94:1
	Twist pitch = 8 D_S	5.0 mm
B.	First Subcable	
	Six copper wires cabled about one core	(6 + 1)
	D_1, uncompacted diameter = 3 D_S	1.39 mm
	Overall Cu to NbTi ratio	26.7:1
	Insulation	Kapton, 0.002 in. thick
C.	Second Subcable (Uninsulated)	
	Six first subcables around a core	6 x (6 + 1) + 1
	D_2, uncompacted diameter = 9 D_S	4.16 mm
D.	Finished Conductor	
	Ten second subcables around a supporting strap	
	Strap dimension	4.5 mm x 13.5 mm
	Uncompacted conductor dimension	13.5 mm x 22.5 mm

cyclic stress amplitude should be well within the expected fatigue limit for properly selected stainless steel.

A contract was awarded to Magnetic Corporation of America (MCA) to produce 534 000 meters of NbTi-Cu composite with the parameters given in Table III, Section A. The wire was shipped to LASL in mid-December. Specification called for the wire to carry 110 A at 4.2 K and 3.0 T at a sensitivity of 1×10^{-12} Ω-cm. All samples tested at MCA have carried between 145 and 156 A under the given conditions. The specification was based on the measured performance of supposedly identical conductor, 1000 m of which had been purchased at the end of 1977.

TABLE IV

30-MJ STABILIZING COIL ELECTROMAGNETIC LOSSES

	Watts
Hysteretic losses due to the transverse component of the changing field	27.0
Hysteretic losses due to the parallel component	3.3
Self-field losses	0.7
Coupling current losses	14.7
Eddy current losses in the (6 + 1) bundle (in case of good bonding)	26.6
Eddy current losses in the copper core	4.4
Eddy current losses in the strap	0.7
Total	77.4

Two thousand meters of first-level subcable were fabricated by MCA. This was split into four 500-m lengths, which were further processed as follows: left as is; soldered; unsoldered, wrapped with 2.5×10^{-3}-cm-thick Kapton; and soldered and wrapped with Kapton. All these first-level cables were then processed into second-level cables at LASL with a core of number 15 AWG copper magnet wire insulated with heavy Formvar. A tension of 6 to 7 lbs was maintained on all seven strands. This gave a high-quality cable with a pitch of 4.57 cm (1.80 in.). In the insulated cables there were no shorts either between the first-level cables or between the wires of the first-level cable and the core. First- and second-level subcables have been subjected to stability tests.

Two contracts were awarded to produce lengths of prototype cable, one for 100 m with Kapton-wrapped insulation and one for 50 m with Mylar-wrapped insulation. As a development step, MCA was asked to produce 100 m of second-level cable insulated with 0.0005-in. Mylar tape applied with 50% overlap. This cable did not pass the insulation test, since it exhibited a short to its metal spool although there were no inter-strand shorts. More important, the insulation was snagged and partly torn in numerous locations. In forming the second-level cable, it may be important to pay attention to the direction of feed of the first-level cable with respect to that of the insulating tape. In

one direction, each turn of insulation presses down the leading edge of the next turn, while in the opposite direction, the leading edge of each turn tends to stand away from the wire, which exposes it to damage. MCA has been asked to process a new length of second-level cable with 0.001-in. Mylar and to pay attention to the feed direction.

Both MCA and AIRCO have supplied samples of composite core, copper stabilizing wire, and soldered and unsoldered bare first-level cable. AIRCO has also supplied a sample of insulated first-level cable. Both manufacturers have experienced difficulty in obtaining and fabricating the 316 stainless steel strap material. During December, AIRCO had a set of rolls ground to the proper profile and had the material rolled to shape after an unsuccessful attempt to fabricate it by drawing. Prototype cable fabrication should begin in mid-January 1979.

Experiments have been completed on mechanical hysteresis losses in the support strap and on the effect of heat treatment upon the residual resistance ratio (RRR) of the stabilizing copper wires. Tests have been initiated on the effect of cyclic fatigue upon RRR and also upon the general mechanical and electrical properties of the conductor. This work is reported in subsequent sections.

Inquiries were sent to seven vendors of fiber-reinforced plastic shapes about the possibility of manufacturing the coil form, the radial spacers, and the conductor support strips. Only two vendors responded that they had immediate capability of manufacturing these items. These were A and M Engineered Composites Corp. and Spaulding Fiber Company, Inc. The center part of the coil form will be a fiber-reinforced cylinder. The end pieces or flanges will be fabricated from laminated, fully characterized, G-10 CR sheet. The superconductor support strips will be machined from G-10 CR sheet. The coil spacers can be made in at least two ways. Filament-wound cylinders could be made and then split vertically into segments or special mandrels could be made and the cylindrical segments could be formed under heat and pressure from B stage G-10 CR.

C. Superconductor Stability Tests (H. J. Boenig, M. Bowden, J. Harlow, R. I. Schermer, W. D. Smith, S. Rose)

In a stability test, heat is supplied to a length of current-carrying superconductor; and the voltage along the conductor is measured as a function

of position and time. The heat is supplied by a heater thermally attached to the conductor and may be either dc or pulsed of variable amplitude and duration. The current carried by the conductor and the background magnetic field applied to it are both parameters that may be varied. This work emphasizes the comparison of experiment with the results of numerical calculations and, in particular, the use of numerical calculations to account for the effect of unavoidable experimental perturbations, such as the special geometry that occurs near the heater. Tests have been run on numerous conductors of varied geometry. In general, it has been found that certain features of the experiment, such as the maximum stable current or the curve of conductor temperature versus heater power, are well represented by the calculation. Fine details are poorly represented and there are some structures in the data that cannot be represented at all by the mathematical model.

Experimental results on BPA conductors are presented here. Three first-level cables were tested under the conditions of being uninsulated and not soldered, uninsulated and soldered, and insulated and soldered. The unsoldered cable gave almost identical results to the soldered cable and is not discussed further. In one series of runs conductors were driven normal with dc power, applied to a 1.1-cm-long heater, just sufficient to produce a normal zone roughly 2 cm long. The bare conductor could carry a maximum current of 280 A in zero field and still recover superconductivity when the dc power was removed, while the insulated conductor could carry only 190 A.

Two measurements were made on second-level cables, which indicated that the insulated wire would carry 85% of the current in the uninsulated conductor. The first measurement was suspect because of shorts between the first-level cables and the insulated support core of the second-level cable and because of various instrumental difficulties. The second measurement, however, has no evident flaws and yet indicates a stability limit of 1250 A for uninsulated conductor and 1150 A for insulated conductor. The detailed data on the uninsulated conductor are unusual. The zones move outward in a stepwise fashion, and there are short-time oscillations in both zone voltage and temperature.

Numerical calculations reproduce very well the data of conductor temperature versus heater power for the bare conductor. The insulated conductor cannot be properly modeled because the thermal conductivity of Kapton is not

known. An illustrative run with Mylar, however, showed no great difference between the expected performance of first- and second-level cables.

The experiments will be repeated. A similar experiment on nylon-covered first-level conductor, performed for the 20-MJ tokamak ohmic-heating coil project by Group CTR-9, showed that an insulated conductor would carry only 65% of the current that a bare conductor would carry.

D. Mechanical Hysteresis Measurements on Cable Support Strap

(R. I. Schermer, J. C. Bronson; D. Eash, CMB-5).

As a preliminary to the hysteresis measurements, tensile tests were performed on specimens of 316 stainless steel and 21-6-9 Nitronic steel. The samples did not have a well-characterized thermal mechanical history, but they were annealed before machining. Comparison of the yield and ultimate strengths of the samples with tabulated results indicated whether the samples were fully annealed. Tabulated data were taken from the handbook compiled by Battelle for ARPA, "Handbook on Materials for Superconducting Machinery." Table V lists the tensile yield strength (TYS) and tensile ultimate strength (TUS) as well as the elongation to fracture (ΔL). The results, by comparison, indicate that the material was fully annealed.

Tests were run on tensile modulus specimens of both steels to look for hysteresis with cyclic loading. Experiments were performed in tension on the Instron machine at 300 K and 20 K. A pair of compensated strain gages, attached to each sample, was arranged to detect any bending moment which might be

TABLE V

TENSILE PROPERTIES OF STRAP MATERIALS

Material	Sample	Temp (K)	TYS (ksi)	TUS (ksi)	ΔL (%)
316	Ref.	300	40	86	60
316	SMES	300	31.5	84	73
316	Ref.	20	97	230	55
316	SMES	20	67.5	250	--
21-6-9	Ref	300	56	100	55
21-6-9	SMES	300	53.5	105	67
21-6-9	Ref.	20	177	241	16
21-6-9	SMES	20	200	254	16

inadvertently applied. The gages were read with an ac-bridge circuit operating at 3800 Hz with lock-in detection and an x-y recorder output. There was sufficient resolution to detect a hysteresis loop corresponding to an energy loss of 0.25% of the maximum stored elastic energy.

No detectable hysteresis was observed provided the cyclic loading was performed within the elastic region. This result applies both to an annealed sample and to a sample which had undergone 0.6% of plastic elongation at room temperature. Work at 20 K was extended to a stress of 345 MPa (50000 psi) and a strain rate of 1.27 cm/min.

In the BPA coil the strap will operate at an average stress of 260 MPa (36 ksi) with a stress amplitude of 45 MPa (6 ksi) peak to peak and a strain rate of 2.54 cm/min.

E. Electrical Resistivity of Stabilizing Copper (J. Harlow, S. Rose, R. I. Schermer)

MCA fabricated 2000 m of first-level cable, which was used in a stability test. The copper used as stabilizer has a residual resistance ratio (RRR) of 250 before processing. The copper stabilizing wire in the first-level cable had an RRR of only 50. The vendor had thought that the tinning or soldering operation would anneal the copper. This did not occur. A vacuum anneal at 315.6°C(600°F) for one-half hour was found to recover most of the low-temperature electrical conductivity; annealing at 426.7°C(800°F) for one-half hour is even better. The related RRR measurements are given in Table VI. Subsequent orders for prototype cable called for annealing the stabilizing copper. The strain in cabling is expected to have only a small effect.

F. Mechanical Effects on Conductor and Fatigue Testing (R. I. Schermer; J. Bennett, Q-13)

The conductor for the 30-MJ stabilization unit will be wound onto a toothed FRP shell. Between the support teeth the conductor passes through an open channel containing liquid helium. In that region the individual second-level cables are subjected to stresses and deflections produced by the magnetic field. A consideration of the forces involved in forming a cable shows that the entire second-level cable should act rather like a solid rod under these conditions and should be able to withstand the forces over the unsupported

TABLE VI

RESIDUAL RESISTIVITY RATIOS OF COPPER WIRES

Sample	Heat Treatment	RRR
A	1	50
B	1	50
C	1	60
A	2	50
B	2	70
C	2	50
A	3	140
C	3	200
A	4	180
C	4	230

A - tinned copper stabilizing wire from first-level cable.

B - same as A except solder removed by abrasion.

C - commercial OFHC.

1 - none; 2 - heated to dull red in air; 3 - 315°C, one-half hour in vacuum; 4 - same as 3 except 425°C.

length. An error in cable manufacture could force each individual first-level cable to support the magnetic force acting upon it; however, calculations indicate that even in an unsoldered cable the outer strands should provide considerable support to the central, current-carrying superconducting strand. Whether or not a cable acts as if made of independent elements or as a solid body depends upon the shear forces in operation compared to the frictional constraints between subcables. It is possible that the friction will produce hysteretic losses, a problem still being investigated. The following facts have been experimentally determined.

1. Samples of both soldered and unsoldered first-level cable, as fabricated by MCA, respond to a transverse load according to beam theory, with the soldered cable being roughly twice as stiff as the unsoldered one. Both were far stiffer than the composite core itself, which acts more like a flexible rope.

2. A sample of second-level cable deflected almost exactly as if its seven sub-elements were acting independently and showed significant hysteresis under large enough loads. It was not clear that strand tension and interfacial friction were maintained in the as-fabricated condition.

The tooth spacing for the conductor support in the BPA coil design will be chosen so that a soldered first-level cable will not be plastically deformed between teeth. The experimental result indicates a spacing of 3 cm is acceptable, but since the stabilizing copper in the test specimen was not annealed, the measurement will have to be repeated.

The possible deflection and bending stress on either first- or second-level subcables were calculated for a variety of assumed end conditions. The actual BPA operating parameters were used and a span between teeth of 1.5 cm was assumed. If the second-level cable acts as a unit, the deflection is less than 1 μm; and the bending strain is less than 10^{-4} in the outer copper fibers. For a first-level cable, the deflection would still only be 20 μm and the strain less than 5×10^{-4} with a cyclic amplitude of less than 10^{-4}.

While it appears that there should be no fatigue effect due to these small deflections and strains, two contracts to study cyclic behavior experimentally have been initiated. J. Ekin of NBS Boulder will study the cyclic affect on the RRR of the stabilizing copper with various samples of materials and first-level cable made by MCA and AIRCO as part of the prototype cable development work. Ekin has already determined that for hard-drawn copper with an initial RRR of 50, there is no effect upon the RRR with a cyclic strain amplitude of less than 0.2%. Ekin will extend this work to both PDOF and OFHC copper with an initial RRR of 250, will look at soldered and unsoldered cables, and will, finally, simulate the actual operating conditions in BPA. This experiment should be complete by mid-January 1979. In the second contract, Van Sciver of the University of Wisconsin will simulate the actual loading on a length of prototype BPA cable at 77 K for 10^7 cycles. This experiment, in the planning stage, will evaluate the integrity of the wrapped insulation.

G. Dewar (J. C. Bronson)

Calculations of cryostat size and various wall and head thickness for the 30-MJ transmission line stabilization unit storage coil have been made.

Fourteen vendors and fabricators of fiber-reinforced plastics were contacted about the possibility of manufacturing the dewars. Four fabricators of fiber-reinforced plastic vessels responded to the inquiry concerning fabricating capabilities. These were TOLO, Inc., Santa Ana, CA; A&M Engineered Composites Corp., Marlboro, MA; Berkeley Cryogenic Associates, Berkeley, CA: and Hasbrouck Plastics Inc., Hamburg, NY.

Hasbrouck Plastics suggested that the cryostat could be fabricated from a semirigid polyester resin system rather than the glass-reinforced-epoxy system proposed in the original inquiry. Berkeley Cryogenic Associates offer, in addition to cryostat fabrication, a Mylar insulation to reduce eddy current losses and a capability for cryostat design.

H. Cryogenic System - Refrigerator (D. B. Colyer, J. H. Fretwell)

A cryogenic helium refrigerator to provide 150 W of refrigeration at 4.5 K plus liquefy 10 liters per hour of helium is on order for delivery in the spring of 1979. Bid requests have been initiated to purchase a trailer to house the refrigerator. Extensive performance and reliability tests will be conducted in 1979. Refrigeration system operating plans are being reviewed to provide a basis for incorporating emergency refrigeration capability and helium gas recovery.

I. Electrical System (H. J. Boenig, R. D. Turner)

The 2.5-kV, 5-kA converter for the BPA unit was designed to guarantee high reliability in the utility environment. The converter is subdivided into two six-pulse, series-connected Graetz bridges, each with a rating of 1.25 kV and 5 kA. For a voltage safety factor of 2.5, as commonly applied in line-commutated converter designs, 3.2-kV thyristors were specified. A maximum ambient air temperature of 50°C and a maximum silicon wafer temperature of 100°C requires six 50-mm thyristors in parallel for an air-cooled converter with an airflow of 1000 feet per minute to carry the full current. Fifty-four duplex assemblies, each consisting of two thyristors with an aluminum heat sink, were purchased for subsequent fabrication into the converter.

A technical specification was written for the 10-MW, twelve-pulse ac-dc converter. An electrical diagram of the ac system, the converter, and the superconducting inductor which makes up the electrical system is shown in Fig. 1. Bids for the converter have been received and a vendor is being selected

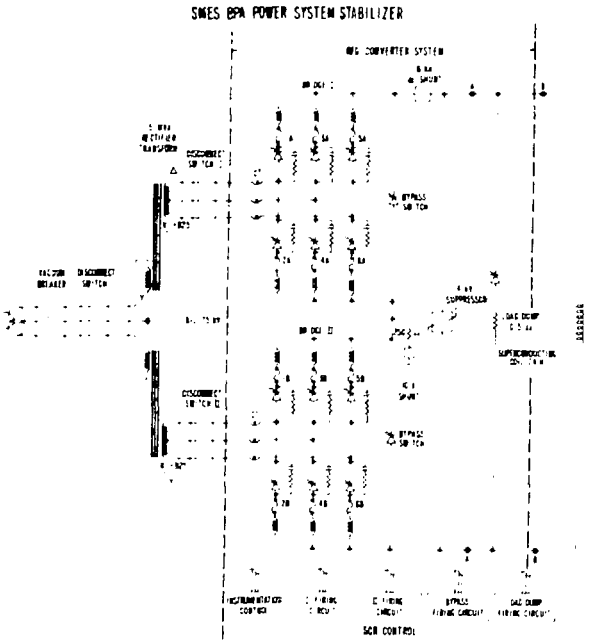

Fig. 1.
The BPA SMES dynamic stabilizer electrical system.

to manufacture the converter. The scope of work includes the system integration, fabrication, assembly, and testing of the twelve-pulse, line-commutated converter.

The converter, as specified, is an ANSI 34.2-1958 standard "Delta, Twelve-Phase, Multiple Delta-WYE Double Way" circuit in which the two three-phase bridges will be operated electrically in series with full-range SCR control. Table VII is a summary of the major electrical parameters of the converter.

J. Purdue Study (H. J. Boenig)

P. C. Krause of the School of Electrical Engineering of Purdue University, under contract with the Department of Energy, Electrical Energy Systems, studied the effects of a SMES unit on the BPA system AC Intertie. The conclusions of the studies were that a SMES unit can damp power oscillations on the AC Intertie and that a 30-MJ 10-MW unit placed at the Chief Joseph Station of the BPA system should be sufficient to damp the power oscillations.

TABLE VII

CONVERTER PARAMETERS

Power (continuous)	12 MW
Single bridge operation	
V_{LL}	928 V, rms
V_{DC}	1250 V
I_{DCmax}	5.5 kA
Speed of response (rectifier-to-inverter mode)	<30 ms

K. Stabilizing Unit Application Study (H. J. Boenig, J. D. Rogers)

The potential use of a small SMES unit for dynamic and transient stabilization of power systems is being investigated by Westinghouse Electric Corporation. Twenty-five electric utilities with potential stability problems were sent a questionnaire to evaluate a SMES device within their system for stability improvement. The report covering the study, including the response to the questionnaire, should be received shortly.

L. BPA Status Summary (L. Cresap, BPA)

BPA has given a status summary of their efforts on the SMES project and some specifics on their planning. The status is as follows.

1. BPA is searching the Seattle area for a switchyard or suitable substation which has a station transformer with an unused tertiary winding and sufficient area to locate a SMES system. If they are successful, this will simplify transformer and high-voltage switchgear needs and will provide a cost savings.
2. BPA is studying the use of the SMES to perform reactive power, load-flow experiments on the northwest power grid. These experiments will be similar to those done with the dynamic brake for the real power load-flow perturbation tests.
3. BPA prefers a digitally controlled algorithim for the control interface to their system . They have adopted the PDP-11 computer as their standard minicomputer.

4. Telephone communication from BPA confirmed their approval of the LASL 10-MW converter design.

III. 1- TO 10-GWH SMES DIURNAL STORAGE UNIT

A. Introduction

A single-point reference design is being formulated for a full-scale SMES diurnal storage unit, sized to operate on a public utility for peak load leveling. The reference design will serve both as a guide for research and development work and as a basis for detailed industrial design of the 10- to 30-MWh prototype unit. The design presents some alternative solutions to previous conceptual studies. These alternatives may be the basis for further development investigations.

B. Electrical System.

1. Converter Design (H. J. Boenig, R. D. Turner). The converter design for the 1-GWh unit was completed. The series-parallel converter switching scheme, as described in LA-7150-PR, is used for the design. This results in the lowest installed converter power and cost. The total converter system consists of two 25-kA 9.0-kV 12-pulse converter modules. Each module is subdivided into four submodules, with a rating of 2.25 kV and 25 kA. A twelve-pulse submodule consists of two parallel-connected six-pulse Graetz bridges, each with a rating of 2.25 kV and 12.5 kA. Each submodule is connected to a 60-MVA converter transformer. Existing SCRs, for instance Westinghouse 77-mm cells, TA 20 series, connected three in series for 2 kV, are adequate in each bridge leg to provide the necessary voltage rating. Four devices in parallel can carry the required bridge current

The maximum reactive power requirement of the converter is estimated to be 150 MVAR. Consistent with HVDC technology, about half of the required VAR can be supplied by the necessary ac filters, the other half can be supplied by static VAR generators. The total cost of the converter system, including the transformers, the Graetz bridges, bypass switches, filter, and VAR compensation equipment is estimated to be $20.5 million. This is based on a unit cost of $40/kW for the converter system and $25/kW for the static VAR generator.

2. Converter (H. J. Boenig). The converter optimization study was completed. Its goal was the development of new circuit configurations for a line-commutated converter to operate with constant power output over a wide current and voltage range. Two circuits for this type of application were analyzed. The module bypass scheme uses a series connection of converter modules, each designed for a different voltage and current rating. Each module is bypassed when the module rating is exceeded to adjust for the constant output power over the full current-voltage range. An optimization procedure was developed to determine the current and voltage rating of the converter modules for the lowest installed converter power. The circuit of a series-parallel module switching scheme was also examined. This circuit allows converter bridges to be switched from a series connection in the high-voltage, low-current mode to a parallel connection when low voltages and high currents are required. Switching occurs without load current interruption in changing from both rectifier and inverter modes of the dc supply. For both schemes an expression for the installed power of the dc supply was derived with the ratio of maximum to minimum current or voltage as a parameter. A patent application has been initiated on the bridge switching scheme.

3. General Electric Converter Design Study (H. J. Boenig, J. D. Rogers, R. D. Turner). A contract was let to the General Electric Company to evaluate costs of different converter designs for large SMES systems. Converters for 1-GWh and 5-GWh SMES units with 4-h charge and discharge rates were evaluated. The cost for the total converter system was determined with the maximum coil current as a parameter. Detailed cost estimates were obtained for the transformer, converter, filter, and VAR compensation equipment. The major findings of the study are the following.

1. Tap changing transformers are not cost advantageous for SMES converters.
2. For a constant power rating and fixed energy exchange, the converter cost decreases with decreasing coil current.
3. Converter cost ($/kW) increases with the charge time for fixed energy exchange.
4. The previously assumed cost ($40/kW) for the total converter station was reaffirmed in the study.
5. Series-parallel module switching was found to be the lowest cost circuit.

The study was done for constant power operation of the magnetic energy storage unit. The total installed converter cost, but not the per-kW cost, can be decreased by operating the unit at low currents at reduced power with constant voltage. This constant voltage mode decreases the voltage requirement of the converter and, therefore, the cost. About 20% saving in total converter cost can be obtained with reduction in the voltage. GE has verbally communicated the per-kW cost of the converter for a 10-GWh unit to be only slightly lower than that for a 5-GWh unit.

4. Bypass Switch (H. J. Boenig). Three modes of operation of a magnetic energy storage unit require a coil bypass switch that gives the current a path other than through the converter. During ac power failure the converter loses its source of commutation and is unable to transfer the current from one set of conducting thyristors to the next one. Since each set of thyristors is rated to carry only one-third of the time, continuous-current conduction would destroy the thyristors. In the coasting mode, when the coil is neither being charged nor discharged, a low-loss bypass switch could eliminate the converter and transformer losses. During a malfunctioning operation of the converter, the coil current can be transferred into the bypass switch. The first two conditions allow a slow, 100-ms current transfer into the bypass switch, the third situation requires a fast current transfer. In the GE study, a thyristor bypass switch is suggested; however, the cost is prohibitively high because it is designed for full converter voltage and current. Preliminary design considerations of an alternative to a thyristor switch show that a series connection of a mechanical switch and diode bank can satisfy the switching requirement. The mechanical switch has to be designed to withstand the maximum coil voltage; however, the switch does not have to break the current. The configuration of diode bank and converter allows, by proper phase control, the current transfer out of the bypass switch into the converter, so that the switch can open in the currentless state. The closing speed requirement of the switch is crucial. Current sharing in the thyristor Graetz bridges after interruption of the primary supply voltage may provide a low-cost bypass switch equivalent. The use of current-balancing inductors in the legs of a Graetz bridge may create the necessary current sharing. The mutual inductance must be small during normal operation to prevent interference between the bridge legs. When the ac supply is not available, the mutual

inductance is increased to induce a voltage greater than the finger voltage of the thyristors to allow thyristor turn-on.

2. Conceptual Structural Design of Large Underground SMES Dewar and Support Struts (J. G. Bennett, Q-13; F. D. Ju, UNM)

Conceptual structural design studies for SMES components conducted during the past year included studies on the outer vacuum vessel structure, the inner helium vessel, the conductors, and the structural supports from inner vessels to the rock. Several concepts for each component were considered, and parameters studied included the effects of various geometric configurations and materials.

During the first quarter of 1978, work on the design of the outer vacuum vessel was completed and the results were presented and published.[1,2] Recommendations were made from an economic evaluation that the outer vessel be based on a design using continuous seam welded plates of aluminum 5083-H38 with a thickness of 2.5 mm and a support spacing pattern of 1 m on centers. Seams should be in the centers of the support pattern to account for the potential annealing of the aluminum 5083-H38 during welding. Point supports are to be designed to accommodate required rock-bolting patterns; but where rock bolting is unnecessary, the rock-bolt shell-anchor concept is to be maintained.

The remainder of the year's work concentrated upon various concepts of inner helium-vessel designs, load-carrying-conductor designs, and rock-to-dewar support designs. The helium vessel was divided to provide a number of separate segments for transmitting the conductor axial force to the dewar and thence to the wall.

In an effort to make use of existing aircraft wing design and construction technology, load-carrying doubly curved dewar designs were considered. These were composed of relatively straight members between supports and used the concept of a stringer and shear web structure covered with a thin skin. The doubly curved box beam carried both the axial and radial components of the conductor loading between supports, but for the very shallow ripples, i.e., large unsupported radii of curvature and small support half-angles, of the relatively straight member, large cooldown thermal stresses occur. This requires that the design be stiff enough that the additive components of the magnetic loading do not cause the design stresses to be exceeded. This situation can be improved by using larger half-angles and smaller unsupported radii of curvature, thus the thermal stress from the straightening during cooldown

are reduced. However, the difficulty of constructing such highly curved members of this cross section makes the concept of questionable value.

Subsequently, the open box beam was investigated, for which the outer wall of the dewar is designed as a doubly curved thin shell, Fig. 2, with a cross section as shown in Fig. 3. Table VIII shows the design parameters, and Table IX shows the resulting design and material costs for a 13-segment dewar of A-304 LN austenitic stainless steel for the 1-GWh concept.

The load-carrying conductor design in the form of a wire rope was briefly investigated. The interstrand frictional losses for such a concept are the biggest unknown and an experimental program will have to be undertaken to measure them before a feasible design can be specified. Structurally, the concept is very attractive. Discussions were held with recognized experts on wire rope. They indicate no data exist on possible frictional heating effects. A wire rope conductor incorporating superconducting wires, stabilizing matrix material, and structural support strands has a considerable mechanical advantage for in-place fabrication with minimal technology development as compared with all other previously conceived conductors for large SMES applications.

In an effort to make better use of the rock structure, a dewar support concept that makes use of "bridges" across the rock tunnel to support the axial magnetic loadings was investigated. The radial component of the magnetic loading was to be carried only to the outer wall. Several problems that make

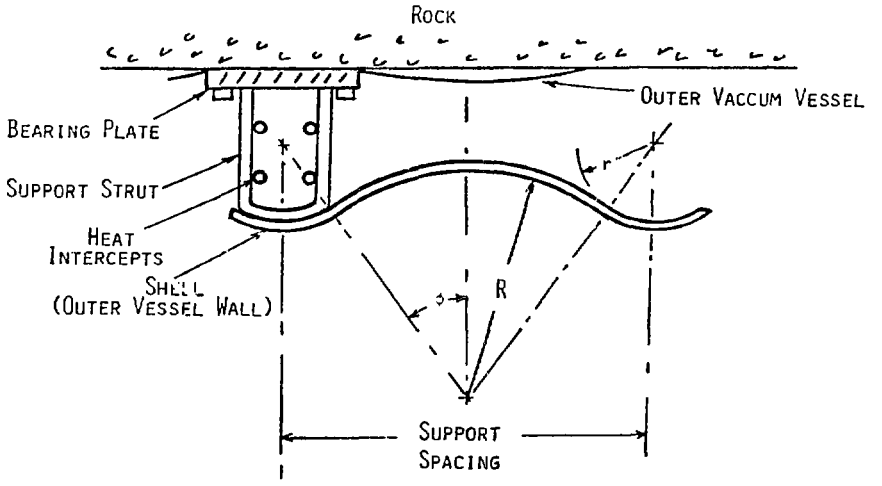

Fig. 2.
Doubly curved shell geometry of the outer dewar wall.

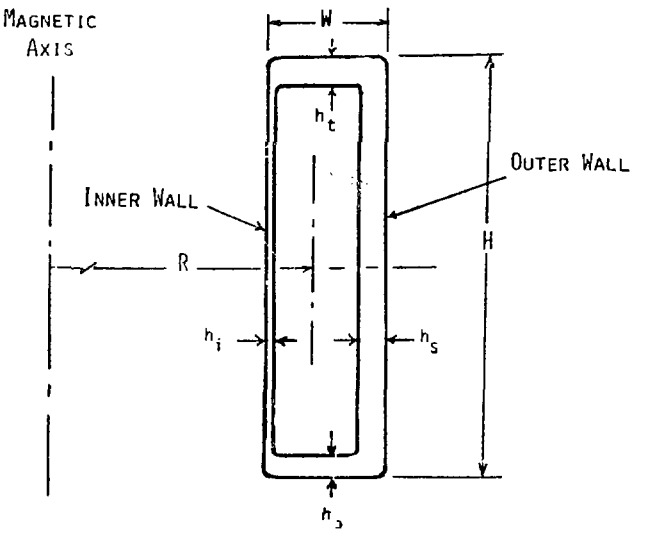

Fig. 3.
Dewar cross section.

this design unattractive are the increased amount of cooling structure material needed for both sides of the axial strut, the additional amount of support material required, the thick load-bearing plates required for both walls, and the radial cooldown motions that must be accommodated at the bridge-strut-dewar interface. The result of this study was that a University of Wisconsin[3] type of vertically running A-frame strut for the outer wall was adopted as the best design concept.

All material is being assembled for inclusion in a point reference design. The reference design will establish a point on a hypersurface from which directions can be taken toward establishing an optimal design.

3. Underground Rock Tunnel Analyses *(R. J. Bridwell, G-6)*

Superconducting magnetic energy storage devices are planned for installation in underground tunnels. Structural supports from the cold inner helium dewar to the 300-K rock make use of the rock as an economical load-bearing material. The rock, from its own weight, is under compression; and the magnetic forces reduce the built-in stresses, in general, to lower compressive

TABLE VIII

INNER HELIUM VESSEL DESIGN PARAMETERS FOR TOP OR BOTTOM END SEGMENT

SMES diameter	132 m
Support spacing	2 m
Dewar width	0.1 m
Design moment at the support caused by the axial magnetic loading	6.3 MN-m
Design shear at the support caused by the axial magnetic loading	20 MN
Material	A-304 LN austenitic stainless steel
Low-temperature design stress	520 MPa
Design thermal strain	3.0×10^{-3}

TABLE IX

A-304 LN STAINLESS STEEL 13 SEGMENT DEWAR

SEGMENT NUMBERS[a]	RADIAL DESIGN PRESSURE (MPa)	DEWAR GEOMETRY							Single Segment Volume of Material (m^3)	COSTS	
		R (m)	(r)	H (m)	ϕ (Deg)	h_i (cm)	h_t (cm)	h_s (cm)		Single Segment 10^6\$	TOTAL 10^6\$
1 & 7	2.5	1.21	0.2	2.2	45	1.0	2.0	1.6	27.6	0.48	0.96
2 & 8	3.7	↓	↓	1.7	↓	↓	9.2	3.4	39.2	0.68	1.36
3 & 9	4.0	↓	↓	1.8	↓	↓	7.2	3.1	37.3	0.65	1.30
4 & 10	4.7	↓	↓	2.0	↓	↓	5.2	2.8	37.9	0.66	1.31
5 & 11	5.4	↓	↓	2.3	↓	↓	3.8	2.5	39.7	0.69	1.37
6 & 12	5.5	↓	↓	2.9	↓	↓	2.4	2.0	42.0	0.73	1.45
13	5.7	↓	↓	18.2	↓	↓	1.0	1.4	203.7	3.52	3.52

[a]Numbers denote inner helium dewar segments with 1 and 7 designating the top- and bottommost segments, and 13, the center segment.

values. Lorentz forces from the energy storage coil cause deformation in the rocks forming the tunnel walls. Elastic analyses of granite under two different dewar load distribution constructions, one with loads on both walls and another with loads only on the outer wall, generate compressive stresses having maximum values of ~270 bars, tensile stresses of ~25 bars, and shear stresses of ~134 bars. These values are ~10% of limiting strength criteria; hence, the tunnels should be stable. However, rock bolting is recommended just below and above the access rooms associated with the vertical coil-dewar tunnel.

Consideration of effects of cyclic loading during the 30-yr history, hydrologic conditions, or locating the dewar in weaker rocks suggests induced stresses may approach failure; and rock bolting for wall stabilization is a necessity.

The mechanical finite element analyses of this report deal with the superconducting coil housed in a 132-m-diam annular tunnel operating at a field of 4.5 T and a storage capacity of 1 GWh. The tunnel geometry is shown in Fig. 4.

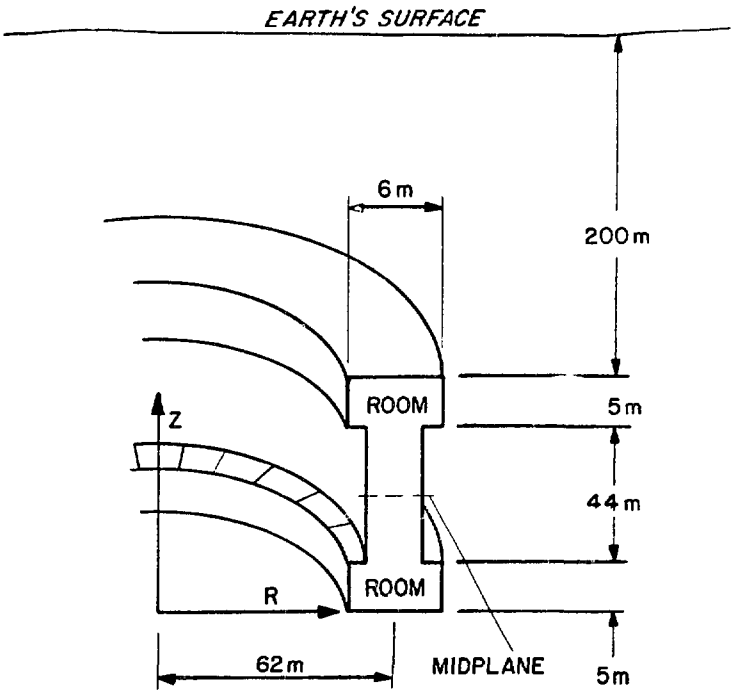

Fig. 4.
Schematic view of quarter section of tunnel designed to contain SMES device.

Since this is a generalized reference design and site selection has not occurred, the strength and behavior of all potential rocks which might house SMES have not been considered. Rock properties for isotropic granite were chosen to allow comparisons with calculations of Fuh et al.[4] for a different tunnel design.

The tunnel for the 1-GWh reference design for the SMES system consists of an annular ring. This annular excavation contains the dewar and supports the cryogenic structure that contains the superconducting coil. The tunnel is a vertical tunnel, 3 m wide and 44 m high, with machinery and access rooms at the top and bottom. The rooms are 5 m high and 6 m wide. Only the portion of the tunnel above the midplane is shown in Fig. 5 to Fig. 13.

The analyses deal with two loading configurations. The first considers the effects of the Lorentz forces, axial and radial, imposed upon both walls. The first dewar segment is physically connected to the walls to take the axial load at a depth of about 3 m beneath the end access room and segments 2 through 6 are attached for a distance about 11 m along the tunnel walls. The axial load support is chosen to set at 45° to the wall. The axial loads are transmitted to the walls as constant axial and radial components botn equal to 59 bars (865 psi). The radial load is a minimum at the top and bottom of the coil tunnel and is a maximum at the midplane of the tunnel. The effect is to increase incrementally the radial load from 25 bars (365 psi) to 57 bars (835 psi) along the entire outer tunnel surface. The radial load term acts in the positive r direction on the outer wall of the tunnel. The radial component from the axial load acting at 45° acts in the positive direction on the outer wall of the tunnel and in the negative direction on the inner wall of the tunnel. Figure 5 is an illustration of the effect of the axial and radial loads.

The second case represents a radical change in the effects of loads on the tunnel. The loads are only active on the outer tunnel wall as shown in Fig. 6. Two major effects are noted in the loads of Fig. 6 relative to Fig. 5. The radial and shear loads from the coil and dewar are applied over distances of 13 m rather 11 m, and the magnitude of these loads has doubled, from 59 to 118 bars. The radial loads from the magnetic field are the same for both cases. The result is to expect larger deflections of the outer tunnel wall for this latter case.

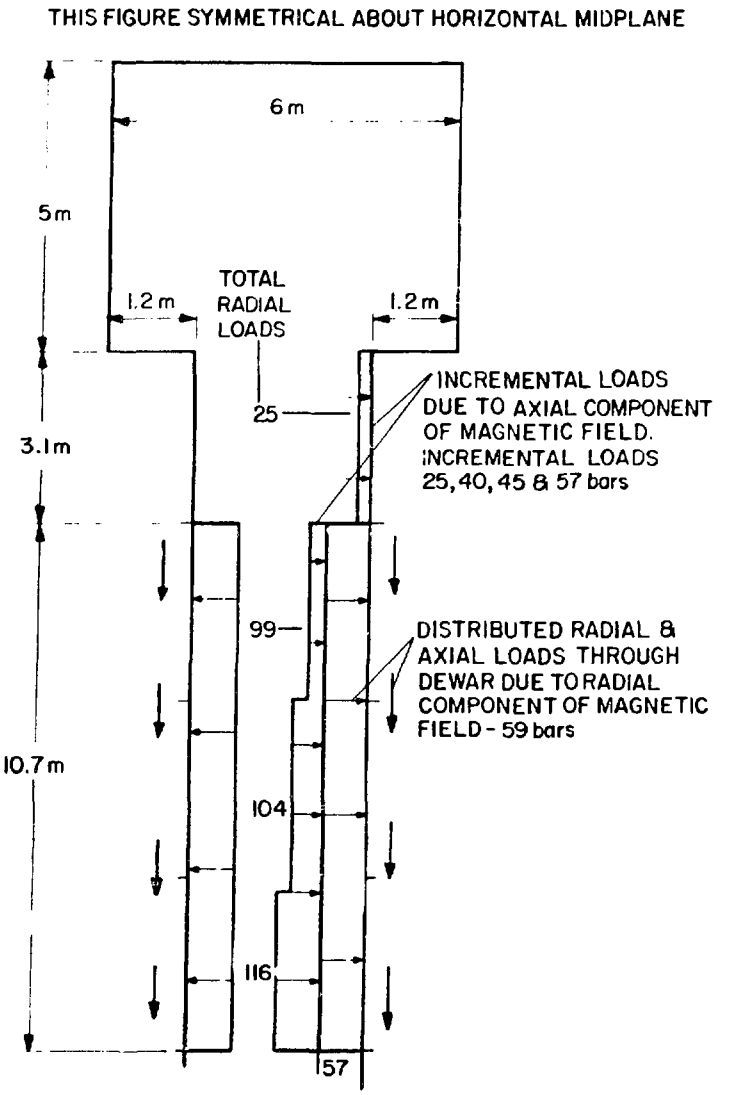

Fig. 5.
Loading system for 4.5-T unit with coil supported by both tunnel walls.

The aspects of site selection require modeling many different rock types, e.g., granite, basalt, limestone, shale, etc. Granite was chosen for this point reference design. The rock properties for granite are assumed to have a Young's modulus of 500 kb (7.5×10^6 psi) and a Poisson's ratio of

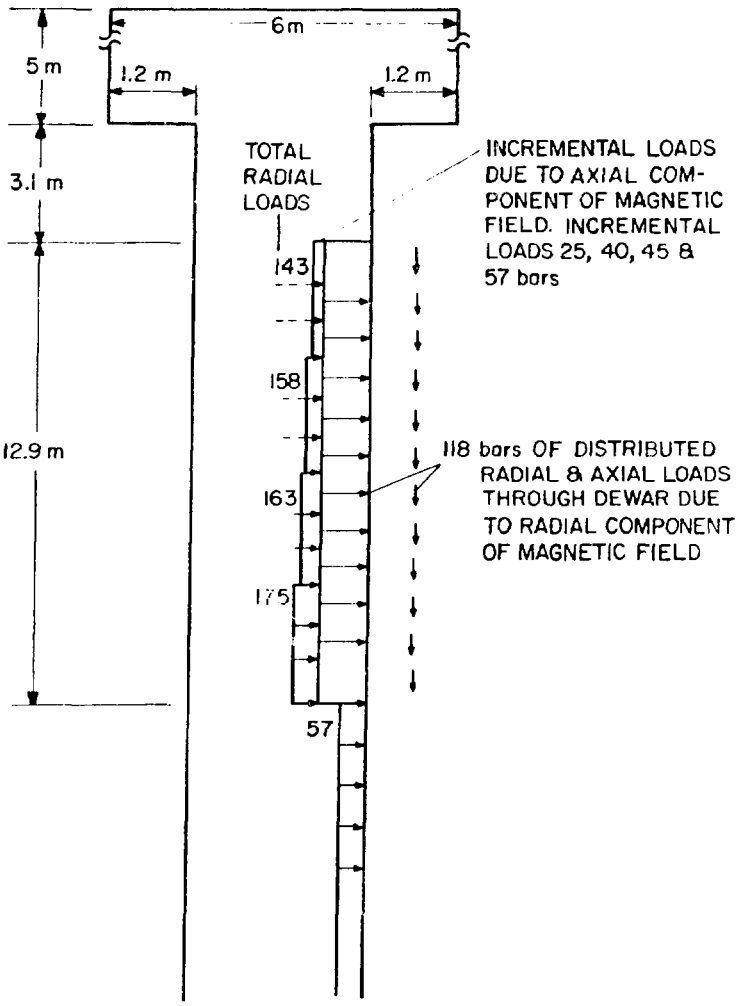

Fig. 6.
Loading system for 5.5-T unit with coil supported by outer tunnel wall.

$\nu = 0.25$. The rock is modeled as an elastic, homogeneous, isotropic continuum. These assumptions allow comparisons of calculated stress levels with other rock properties from handbooks[5] to determine the initial stability of the tunnel to first loads. Because of the paucity of properties for long-term fatigue under cyclic loading, effects of joints on the rocks, interaction of the hydrologic environment, and other considerations, the stability calculations are biased toward instantaneous steady-state models. Long-term considerations will increase the probability of tunnel instability.

The maximum radial load for the first case with the dewar support taken on both tunnel walls is 112 bars, and the radial displacement is 0.4 cm (0.2 in.). Maximum deflection occurs at the 18.8-m level from the very top of the excavation on the outer tunnel wall.

The maximum principal compressive stress is slightly greater than 155 bars (2250 psi) at 15 m below the access room. Stress contours are shown in Fig. 7. No tensile stresses occur when the axial loads are applied to both sides of the tunnel. The minimum principal stress is compressive as shown in Fig. 8. The maximum principal stress is in a plane in which there is no shear, and the minimum principal stress is at right angles to the maximum principal stress. The negative sign notation in the figures indicates compressive stresses.

The hoop stress has a maximum value of 56 bars (~840 psi) between the centerline of the tunnel and the inner tunnel wall as shown in Fig. 9. Shear stresses reach maximum values of 74 bars (~1110 psi).

For the second case, with all the loads on the outer tunnel wall with a maximum radial load of 175 bars, the displacement becomes as large as 0.7 cm (0.3 in.). The region of this large deflection occurs ~10 m below the access room and extends downward to the midplane. The displacement increases somewhat along the outer wall toward the midplane.

The maximum principal compressive stress is 269 bars (~3900 psi) occurring ~20 m below the top of the room as shown in Fig. 10. Zero compressive stresses occur within the tunnel. This shows on most of the figures and is an artifice of the computer code. The minimum principal stress is compressive, with the exception of a tensile region of magnitude 22 bars (~330 psi), located between 205- and 210-m depth shown in Fig. 11.

The hoop stress is generally compressive except in the region of the intersection of the vertical tunnel wall and the access room. This tensile hoop stress of 13 bars (~220 psi) is shown in Fig. 12.

A maximum shear stress of 134 bars (~1950 psi) occurs at the bottom of the dewar support along the outer tunnel wall. Fig. 13 shows the increasing range of shear stress approaching the 220-m depth. For the case with all the support on one tunnel wall the load near the access room has been decreased by increasing the vertical height of the tunnel. In Fig. 6 there is no load above the first 3.1 m of tunnel wall.

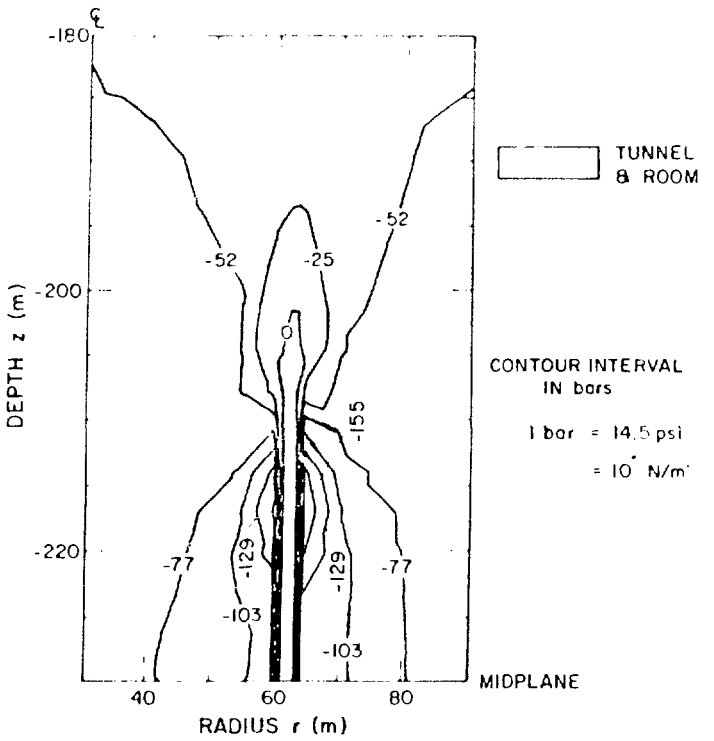

Fig. 7.
Maximum principal compressive stress with coil supported by both tunnel walls, maximum stress 155 bars.

Rock stability criteria are usually based on uniaxial compressive strength measurements. For granite, the compressive strength[5] is ~2-4 kb. Tensile strength is generally related to compressive strength by the rule-of-thumb that $S_T = 0.1\ S_C$; hence, tensile strength would be in the range 0.2 to 0.4 kb. Shear strength is related to compressive strength by $S_S = 0.5\ S_C$; hence, shear strength would have the range 1 to 2 kb.

The second case study, due to larger loads on the outer tunnel wall, gave the larger stress levels. Compressive stresses have a maximum of 270 bars, tensile stresses range from 22 to 27 bars for the radial and hoop stresses, and the maximum shear stress is 134 bars.

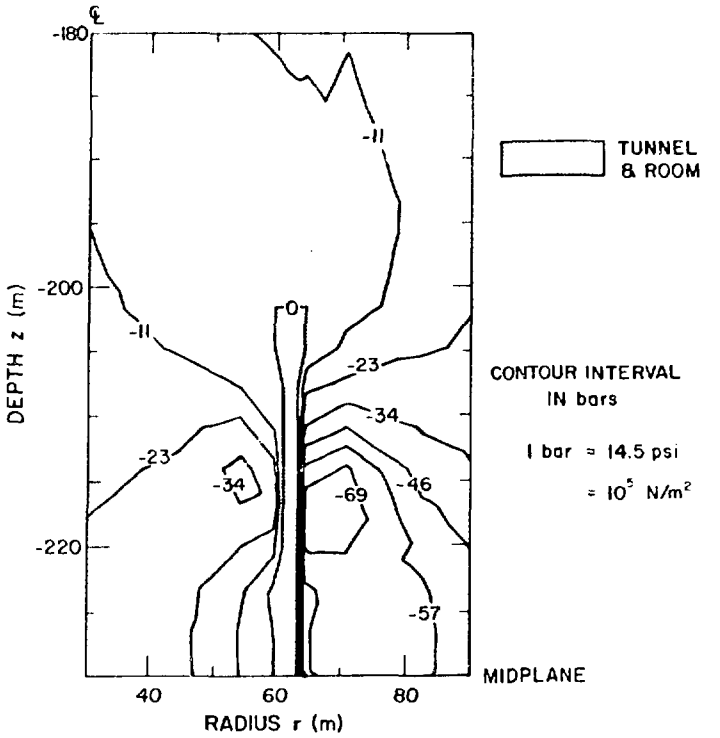

Fig. 8.
Minimum principal compressive stress with coil supported by both tunnel walls.

Comparison of the calculated stress systems with stability criteria from rock mechanics measurements indicates that calculated values are only a maximum of 10% of all criteria. Therefore, these calculations indicate that the imposition of the dewar loads on the outer tunnel wall will not cause failure if the tunnel is mined in granite.

Although the tensile and shear stresses are considerably less than the strength criteria, the engineering safety technique of rock bolting is clearly needed. These calculations indicate that rock bolting is needed at the top and base of the vertical tunnel wall to eliminate tensile stresses. They also indicate rock bolting will be needed at each region that has axial force supports nearest the midplane of the tunnel; i.e., for segments 6 and 12 in particular.

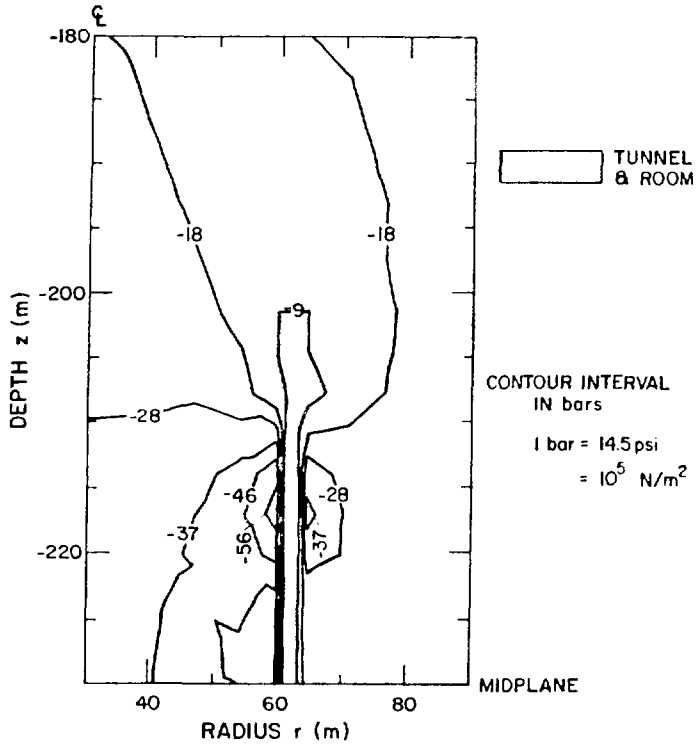

Fig. 9.
Hoop stress with coil supported by both tunnel walls.

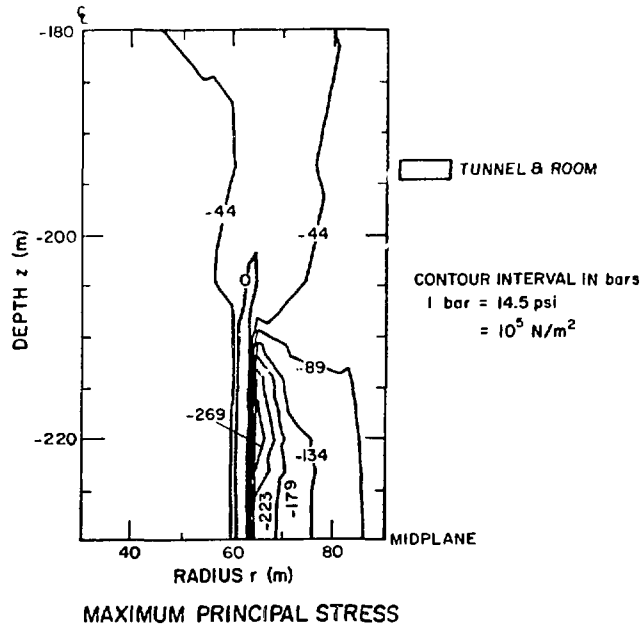

Fig. 10.
Maximum principal compressive stress with coil supported only by outer tunnel wall, maximum stress is 269 bars.

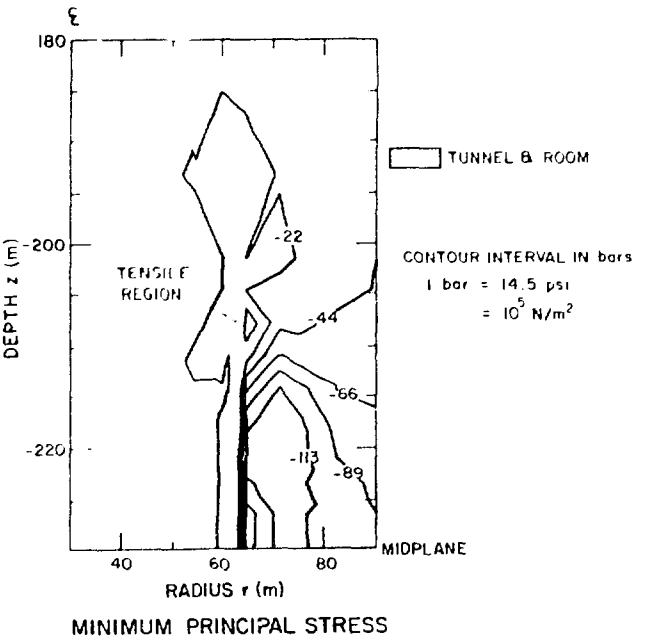

Fig. 11.
Minimum principal compressive stress with coil supported only by outer tunnel wall.

The preceding elastic models ignored cyclic loading of the magnet for 30 years, effects of joints in the rock mass, interaction of the hydrologic environment on rock strength, and ground motions due to nearby large earthquakes. Although data on the first three items is really very sparse, limited research suggests that each contributes to a decrease of the stability criteria. If this decrease is as much as an order of magnitude, it is not at all clear that such a structure is feasible.

If the rock type chosen for the tunnel site has smaller strength criteria, e.g., dolomite, limestone, or shale, then the loads used here may violate stability criteria in the weaker rocks. The first three items would tend to increase the failure probability for the weaker rocks in a more drastic fashion. Creep models should be directed to evaluate the cyclic fatigue behavior of host rocks. Rock-mechanics studies are necessary to ascertain coefficients of strength for the creep constitutive laws. Related measurements of interactive effects of pore pressure and fracture are strongly needed as well. The

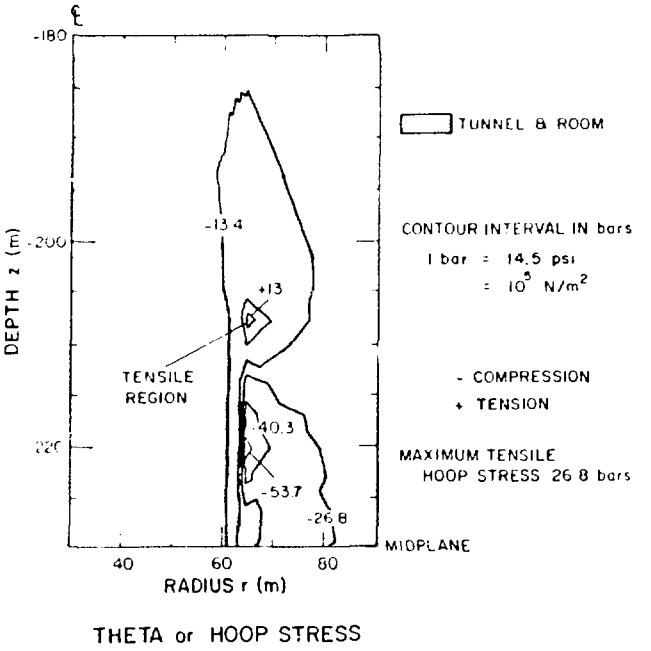

Fig. 12.
Hoop stress with coil supported only by outer tunnel wall. Tensile stress of 27 bars occurs in region just below access room.

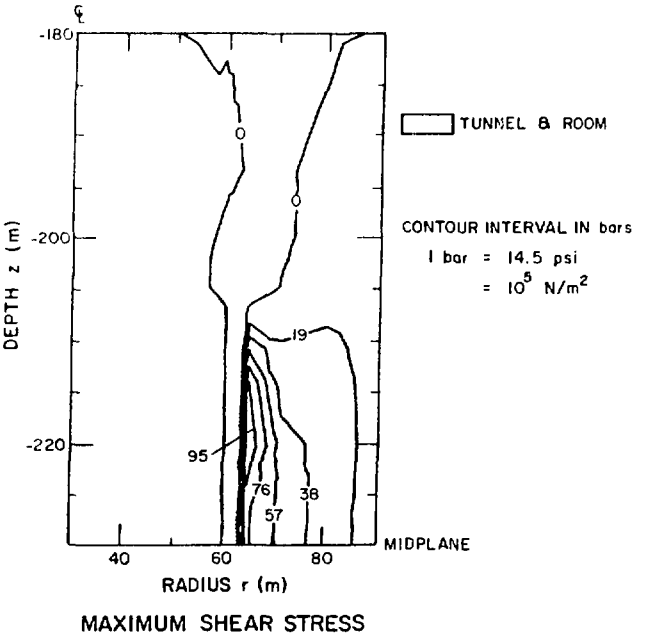

Fig. 13.
Maximum shear stress with coil supported only by outer tunnel wall. Maximum value of shear stress is 134 bars at 220-m depth.

uncertainties presented here must be resolved in any specific SMES tunnel construction; and in the absence of their resolution, extensive rock bolting will be necessary.

The rock-mechanics analyses were performed for locating the storage coil at depths of 200, 300, and 500 m. This parameter was considered to determine the minimum depth where significant tensile stresses begin to develop in the rock structure with application of the loads resulting from charging the coil. The tensile stresses at 200 m are sufficiently small to be of little concern if rock bolting is used. To locate the coil at any depth less than 200 m would increase the tensile stresses to undesirably larger values. Only the 200-m depth results are presented here.

4. Tunnel Excavation and Construction Cost Study (J. D. Rogers; Ed Armstrong, Fenix and Scisson, Inc.)

A consulting contract was placed with Fenix and Scisson, Inc., a mining engineering firm, to make a SMES tunnel excavation and construction study and to obtain costs for same. The tunnel conforms to the configuration of Fig. 4. The study considered locating the coil and dewar at the depths of 200, 300, and 500 m. Only the cost estimates for the 200-m depth are presented here.

The excavation called for six 1.82-m-diam drill holes with steel linings for vacuum pump-out lines; a production shaft, 3.96 m by 3.35 m with concrete-lined stabilized walls and a skip hoist for subsequent use in assembling the storage coil; a horizontal shaft, 3.7 m by 3.7 m, extending 250 m horizontally from the center line of the tunnel axis to an equipment room at the 227-m level; and an equipment room, 20 m by 20 m by 10 m high, with its own 3.9-m by 3.9-m vertical service shaft.

The rock walls throughout the excavation are to be stabilized with rock bolts. The main storage coil tunnel is lined with impermeable load-bearing concrete walls with a minimum compressive strength of 422 to 563 kg/cm^2. Steel load-bearing plates are mechanically anchored to both walls with 50-mm-diam by 1-m-long zinc-plated rock bolts. The zinc plating is required for a 30-year life. Twenty-five-millimeter copper pipes on 1-m centers are imbedded in the concrete lining of the tunnel walls. These supply heat to prevent freezing of the concrete from the dewar heat leak. Provision was made to remove ground water seepage from behind the tunnel concrete wall lining. The underground equipment room was found to provide a saving in the refrigerator

system. Its remote location from the coil was necessary to have the equipment in a low fringe field of 200 G for maintenance.

Subsequent analysis and design changes, e.g., locating the vacuum pumps in the equipment room and adoption of a single tunnel wall support system for the storage coil, enabled several simplifications. These were principally the elimination of the six drilled shafts, provision for the production shaft to also serve as the equipment room access shaft, thus eliminating one vertical shaft, elimination of the 25-mm copper pipes in one wall, and a lower quality concrete on the inner tunnel wall. Associated savings are estimated to be 12.1 to 15.0 millions of dollars. This reduces the original Fenix and Scisson cost from $48.5 to from $33.5 to 36.4 million. The first number corresponds almost exactly to the high-end estimate quite recently done on an independent basis for the University of Wisconsin for a 1-GWh system. The LASL excavation-construction specifications carry the tunnel preparation to a more advanced state for dewar and coil installation and includes details for 30-year life, e.g., zinc-coated rock bolts, and for such items as ground water seepage. For these reasons, one can expect a somewhat higher cost.

5. Refrigeration System (D. B. Colyer)

The refrigeration system provides the liquid helium and cold gas to the cryogenic system to cool the storage coil at 1.8 K and to distribute cold helium gas to the support struts and dewar radiation shield. The refrigeration system consists of the four major subsystems -- the helium compressors, cold box, low-pressure pumps, and helium storage facility. Helium gas is compressed to high pressure and piped to the cold box in the underground equipment room, where it is cooled by heat exchange and energy extraction. The resulting liquid helium is piped at 4.2 K to the dewar, where it is expanded to 1.8 K and 12.5 torr (0.0165 atm) in an evaporator heat exchanger within the storage coil dewar. The evaporator absorbs heat from the liquid helium bath surrounding the coil to maintain the coil at approximately 1.8 K at a pressure of 1.0 atm. Low-pressure vapor from the evaporator is returned to the cold box. Some of the 4.2 K liquid cools the power leads. This liquid is vaporized by the power leads and is returned to the compressors at approximately 300 K.

Secondary heat loads consisting of support struts and the dewar heat shield are cooled with 18-atm helium gas from the cold box at nominal temperatures of 63 K and 12 K. A 10.0 K temperature rise in the helium is allowed, and it is then returned to the cold box.

Low-pressure helium pumps provide the continuous pumping or suction head necessary to pull the 1.8 K, 12.5-torr helium gas through the transfer line and cold box for heat exchange and then raise the warmed 300 K gas to 1 atm pressure to feed the main helium compressors.

With the coil dewar 200 m below ground level, the gravity head represents a substantial part of the 12.5-torr pressure drop available from the heat-exchange evaporator in the coil dewar. Under these conditions the refrigerator cold box should be located at the same level as the coil dewar to warm the return gas. Locating the low-pressure pumps at ground level is costly; so they and the cold box will be placed underground in the equipment room. The cryogenic transfer lines are to run from the cold box in the horizontal drift or tunnel connecting to the dewar. High-pressure helium supply gas from the compressors to the cold box and low-pressure return gas from the cold box and pumps to the compressors will be at 300 K. The warm gas pipe lines will be run in the vertical production shaft.

6. Vacuum System (J. C. Bronson)

In design of the cryostat vacuum system the original concept was to locate the pumping stations at ground level and to run downcomers to the cryostat, which was at a depth of several hundered meters. Three designs were made; however, once the cost of drilling shafts for the vacuum lines was known and the cost of the large stainless steel pipe was obtained, these designs were abandoned. Six alternate arrangements with the vacuum equipment at the dewar level were proposed. The equipment arrangement finally chosen consists of pairs of diffusion pumps equally spaced around the circumference of the cryostat at the lower edge. The mechanical blower and roughing pumps will be located in the underground equipment room.

Careful attention has been given to specifying equipment that is both economical and reliable. Costs for the main components--pumps, piping, valves, and instrumentation--have been obtained.

7. Aluminum-Stabilized Conductors (J. D. Rogers, R. I. Schermer).

Previous studies of large SMES units for diurnal load leveling have stated that such systems will be far more economical if high-purity aluminum

is used as a stabilizer. Although the conclusion may not hold if coil protection controls the design, the development of aluminum-stabilized conductors has been pursued along two lines. First, a contract was awarded to AIRCO Superconductors, Inc., to fabricate short lengths of rectangular conductor consisting of high-purity aluminum jacketed by copper for protection. An analytical study shows that such a conductor should have excellent transverse load-bearing characteristics. AIRCO has fabricated several varieties of the conductor, all with cross-sectional area of roughly 0.2 cm^2, with different copper fractions, copper hardness, and conductor aspect ratio. AIRCO has measured the RRR, minimum bend radius, and tensile strength on each sample and has performed metallurgical analyses. To date, only one sample has been received. This is an 8-cm-long length of material with the following properties: aluminum, 77 vol %; RRR = 1684; TYS = 35.3 MPa (5.1 ksi); TUS = 117.2 MPa (17 ksi); dimensions 2.8 mm x 7.0 mm.

Second, a contract was awarded to ALCOA to perform a cost study of high-purity aluminum production to be based upon the results of proprietary pilot plant results. The study has been received. Cost information is supplied for aluminum with a purity of 200, 2000, and 5000 RRR. Two production situations were used for each purity: (1) 1 x 10^6 kg/yr production rate with a 30-yr sustaining market and (2) 1 x 10^6 kg/yr production rate for two years only. The cost study results are presented as ranges and include the selling price of the aluminum for each case; cost of facilities including construction, engineering, and related costs; the cost of money and depreciation (interest/amortization); and energy costs, the total of power and fuel. The ranges are affected by possible production variations and other uncertainties that are discussed. Information is also given on plant location options and the preferred feed to the purification facility with ore-source effects.

The results of the study indicate that extreme purity aluminum can be produced and sold for much lower prices than the current market situation would indicate. At present, 2000 RRR material costs $40/lb in unfabricated form. The prices for the 30-yr sustaining market case are given in Table X.

8. Influence of Protection Requirements on Costs (R. I. Schermer)

An analysis was made to determine the effect upon SMES economics of the requirement to protect the coil, that is, to remove rapidly all or part of the stored energy in the event of an emergency. New results were obtained when

TABLE X

COST STUDY SUMMARY, 30-YR MARKET, PRODUCTION 1 x 10^6 kg/yr

Purity Cases	200 RRR Aluminum	2000 RRR Aluminum	5000 RRR Aluminum
1. Investment (million $) (Cost of Facilities)			
(a) Construction	2.3-3.4	8.1-16.2	12.0-36.0
(b) Engineering	0.3-0.4	1.3-2.6	1.7-5.1
(c) Working Capital	0.2-0.3	0.8-1.6	0.8-2.4
(d) Startup Expense	0.1-0.2	0.5-0.1	0.7-2.1
Total	2.9-4.3	10.7-21.4	15.2-45.6
2. 10% Interest/Amort.			
$/kg	.44-.66	1.65-3.30	2.33-7.00
($/lb)	(0.20-0.30)	(0.75-1.50)	(1.06-3.18)
3. Power and Fuel Costs (Purification only, no smelting)			
$/kg	0.20-0.29	0.55-1.10	0.79-2.38
($/lb)	(0.09-0.13)	(0.25-0.50)	(0.36-1.08)
4. Sales Price			
$/kg	2.60-4.00	6.60-19.80	8.80-44.00
($/lb)	(1.20-1.80)	(3.00-9.00)	(4.00-20.00)

the turn-to-turn voltage V, during discharge, was taken as the controlling parameter. This potential difference determines the allowable current density j in the conductor matrix and the matrix volume according to the relation

$$V = j^2 E / f(\Theta)(NI)_o \quad , \tag{1}$$

where

$$f(\theta) = \int_o^{\Theta} \frac{\partial C}{\rho} \, dT \quad , \text{ and} \tag{2}$$

E is the energy to be removed from a coil with $(NI)_o$ ampere-turns, ∂ is the conductor stabilizer density, C its specific heat, ρ its resistivity, and Θ the maximum temperature to which a point in the conductor is allowed to rise. Usually, thermal stresses limit Θ to < 100 K.

Table XI lists the fabricated stabilizer cost for the 1-GWh SMES reference design under various sets of assumptions involving ε, the fraction of energy to be removed; the allowable voltage per turn; and the stabilizer material, either copper or aluminum.

For aluminum, this restriction on j is quite severe. From stability considerations alone it appears that a conductor using 2000-RRR aluminum and 1.8 K cooling, which would be cryostable at close to 100 kA/cm^2 and would cost \$1 x 10^6, could be designed. On the other hand, it is fairly difficult to design a practical cryostable copper conductor that operates at 20 kA/cm^2.

Note that $f(\Theta)$ contains all the material properties and, in particular, the allowable heat flux into the liquid helium does not appear in Eq. 1. If the voltage per turn is, in fact, the controlling parameter, it is impossible to reduce the conductor volume by taking advantage of better heat transfer or lower resistivity.

9. Load-Bearing Capability of the Conductor (R. I. Schermer; J. G. Bennett, Q-13)

The transverse load-bearing capacity of a rectangular conductor model composed of a hard copper shell surrounding a soft, high-purity aluminum core was analyzed. An optimum shape and minimum copper fraction for the conductor to carry a maximum load, subject to the simultaneous constraints that both the

TABLE XI

CONDUCTOR STABILIZER COST FOR 1-GWh SMES COIL PROTECTION

ε	V (V/turn)	Material	j (kA/cm^2)	Cost (\$ x 10^6)
0.01	100	Cu	21	13
0.01	100	Al	15	11
0.10	100	Cu	6.6	40
0.10	100	Al	4.7	34
0.01	1000	Cu	66	4.0
0.01	1000	Al	47	3.4

copper and aluminum are strained to the desired degree, was found. The problem is dominated by bending in any copper side walls that are not supported transversely. If conductors are arrayed side by side, this condition only occurs in the outermost walls. The load can be maximized by making the conductors short and wide and by using a copper fraction of about 50 vol %. A far better solution is to use a heavier strip of copper or aluminum alloy along the outer edge of the entire conductor stack to provide support against bending. In this case the conductors should be relatively tall and narrow. A conductor stack with 25 vol % copper, with stiffening strips, should be capable of supporting 11.5 ksi of vertical pressure while producing 0.1% strain in the soft aluminum.

10. Coil Design (R. I. Schermer; P. Thullen, CTR-9)

Magnetic fields and forces resulting from a spatially uniform current density for the 1-GWh reference design coil were calculated. The field at the inner radius and axial midplane is 4.16 T, while the field at the average radius and coil end is 6.5 T. The radial pressure varies from 4.03 MPa at the ends to 5.21 MPa at the midplane. The total axial stress, if accumulated at the midplane, would be 462 MPa. If the axial force is removed to external supports when it accumulates to 69 MPa, there would be a self-supporting central section 18 m high flanked by six sections on each end with supports to the rock cavity wall. The top and bottom coil-dewar sections would be 1 m high.

As an alternate scheme, the current density was varied as a function of axial position to flatten the field and remove the field peak at the coil end. The resulting coil has a field that is 4.5 T at the inner winding and axial midplane, is constant to 1% over the central 95% of the axial length, and decreases to 4.3 T at the ends. The radial pressure is 5.79 MPa at the midplane and decreases to 1.45 MPa at the ends. The total accumulated axial stress at the midplane would be 503 MPa. Again, by accumulating a maximum axial force of 70.5 MPa, the central section is 18 m high flanked by six sections on each end, with the outermost end sections 1.7 m high. The spacing of the dewar-coil sections is rather uniform. In contrast with the uniform current density model, this coil requires less superconductor, less radial support, more axial support, and probably costs almost the same amount. It offers a useful option for the geometrical arrangement of the supports and is the basis for the work reported above.

IV. ANALYTICAL STUDIES

A. Subsynchronous Resonance SMES Coil (B. Turck)

The possibility of using a superconducting coil to stabilize the subsynchronous resonance of an ac generator has been investigated. It has been seen that a 5-MW storage coil operating at a frequency of 50 Hz is quite feasible. The condition of using a cryostable conductor with losses as low as possible lead to an optimization of such a coil. To study the influence of the different parameters, a Brooks coil was chosen to work out simple calculations. The results are quite general and can be extended to any coil shape. For the sake of comparison, three kinds of conductors were investigated: a monolithic conductor, a cable made in one stage, and a cable made in two stages. The results are not very different and must be analyzed in detail. Typical parameters for such a coil are listed in Table XII.

Two major results are found as follows.

1. A monolithic conductor can be used with low losses at a frequency of 50 Hz by increasing the twist pitch.
2. The hysteretic loss decreases with increasing radius as the first power and the eddy current and coupling loss decrease with increasing radius as the fifth power. Losses can be reduced to an acceptable level at the cost of increased radius, increased stored energy, and increased conductor volume.

TABLE XII

SUBSYNCHRONOUS RESONANCE SMES COIL

PARAMETERS

Voltage	8 kV
Current	1 kA
Stored energy	2 MJ
Current density in coil	22 A/mm^2
Loss power	350 W

B. Propagation Velocity of a Normal Zone in a Superconducting Composite

(B. Turck)

Various propagation velocities of a normal zone have been given by several authors. In these theories the current sharing region is not taken into account. Different initial assumptions can lead to discrepancies among these expressions. A new expression is proposed that, in particular, gives the correct values of the full recovery and cold-end recovery currents, together with an exact and finite propagation velocity when the transport current tends toward the critical current. In the case of poor cooling the velocity is shown to be independent of the heat transfer, and it depends only very little on the physical properties of the conductor. There is almost no difference between a copper matrix and an aluminum matrix. The velocity decreases with increased cross-sectional area. Moreover, for small currents the velocity is proportional to the current. Then, as the current increases, the velocity increases more rapidly than in direct proportion to the current. Finally, the velocity, as the transport current reaches the critical current, tends to a finite limit proportional to the critical current.

C. Filament Shielding Effects on AC Losses (B. Turck)

A report has been written on the losses in a multifilament superconducting composite submitted to an external changing field for three basic cases -- a slow-rate triangular wave, a single-shot exponential wave, and a sinusoidal wave. Account is taken of the saturation of the outer layers of the filaments arising from the coupling currents. Complete expressions are provided. In most cases simplified expressions may be used. The existence of two kinds of induced currents in the matrix--coupling currents between the filaments and eddy currents--is treated. The overall losses are not calculated by an addition of both contributions but by a combined effect directly related to the respective time constants. It is particularly interesting to note that in the case of a high-frequency sine-wave field, the hysteretic and coupling current losses are almost negligible due to the shielding effect and can be decreased to a very low level by increasing the twist pitch length of the composite.

V. EXPERIMENT TO MEASURE CURRENT SHARING BETWEEN STRANDS IN A CABLE MADE OF INSULATED STRANDS (H. J. Boenig, M. Bowden, D. O. Harkleroad, R. I. Schermer, B. Turck, W. D. Smith).

Several tests were made to determine current sharing and response times for a multistrand cable wound into a coil. A number of combinations of strands were powered in a controlled manner and individual diagnostic measurements were made.

In a first experiment only three strands out of eleven were supplied with current, and the current distribution was unequal. The ratios between the initial currents were 0.83, 1.0, and 1.25. The calculated values were 0.69, 1.0, and 1.37. The shapes of the curves clearly indicate the existence of two time constants. The longest could be measured and was equal to the calculated value to within 15%. Thus, it is possible to calculate the various mutual inductances between the strands in a cable with a fairly good approximation. It is shown that the current distribution depends only on the differences between the $L_i - M_{ij}$ values.

In a second experiment, the current sharing was also studied for the case of a quench occurring in one of the strands. The current is transferred to the other strands after a time function dependent on the electromagnetic time constant $(L_i - M_{ij})/\sum(R+r_i)$ and on the lifetime of the normal zone.

In a third experiment, only a bundle of five strands was supplied with current. In agreement with the calculations, the center wire did carry a current in the direction opposite to the main current. This is merely due to the fact that the self-inductance of the center wire is just a little smaller than the inductance of the other wires, but that is sufficient to produce a huge and catastrophic effect. The time constants and amplitudes of the currents were also in good agreement with the predictions.

VI. SUPERFLUID CRYOSTATS (D. B. Colyer, M. D. Henke, R, I. Schermer, D. O. Harkleroad, J. F. Taylor, W. D. Smith)

Two cryostat systems, capable of operating at 1.8 K and 1.0 atm, were designed for heat transfer and conductor stability experiments. One system is a small system capable of cooling 8.2 liters of helium. The first test

results provided 2.45-W refrigeration at 1.8 K. The second system will provide about three times this refrigeration at 1.8 K. This is to be accomplished with a larger low-pressure pumping system to be delivered in early 1979.

VII. ALTERNATIVE SMES APPLICATIONS

A. Subsynchronous Resonance Control (H. J. Boenig)

The use of a small SMES unit (~3 MJ) for subsynchronous resonance (SSR) damping was studied. Several schemes, such as static filter, modulated resistor, modulated inductor, and dynamic filter with cycloconverter have been proposed to damp SSR instabilities. A new scheme was suggested which uses a storage inductor and two converters to control SSR. This has the advantage that it can couple two independent systems together and exchange power between them. It is also applicable to generation systems in which pulsed power is generated and the average of the pulsed power is transmitted into the distribution system.

B. Regenerative Braking for Freight Locomotive (R. D. Turner)

A study was made to evaluate the technical feasibility of a SMES unit as an on-board energy storage device for use by freight locomotives. For this application, a SMES unit appears capable of providing a substantial energy utilization benefit by providing a means of storing a train's change in momentum in a superconducting coil. This stored energy could be reused for traction-motor propulsion power as opposed to its being dissipated as heat by the conventional resistive dump and mechanical braking systems. Dynamic systems provide braking force by connecting the traction motors as separately excited generators that provide brake loading proportional to a combination of their field excitation, armature rotational (track) speed, and train operator control.

In this study, a 100-car, 8520-ton freight train was assumed. Rolling losses were based upon the universally accepted Davis formula for calculating a train's rolling resistance, which is as follows:

$$R = 1.3 + \frac{29}{W} + 0.045^{*}V + \frac{0.0005^{*}AV^{2}}{Wn}$$

where R = resistance in lbs/ton on level tangent track

W = weight per axle in tons

n = number of axles per car

A = cross section of car in square feet

V = speed in miles per hour.

The first two terms arise from the journal losses, the third from the wheel flanges, and the last from windage losses. The rolling losses and those due to the circuit and traction-motor losses are subtracted from the potential energy due to change in grade to obtain the available train braking energy for storage.

Figure 14 shows the energy available for storage and transfer inefficiencies, after deducting the rolling losses, displayed as a function of speed with parametric percent grade curves. The graph is for downgrade operation of a 100-car train.

Preliminary sizing of superconducting energy storage coils that might be considered feasible, based on overall current density of 2 kA/cm^2 and a central field of 5T, shows that approximately 450 MJ of energy could be stored in a solenoid 2.4-m mean diameter by 15 m long. With energy storage of 450 MJ, 400 MJ can be assumed as usable. This corresponds to 110 kWh of reusable energy. Other configurations and specific road-bed profile information are being evaluated to evaluate SMES for locomotive applications.

VIII. MISCELLANEOUS

A. 3.25-MW ac-dc Power Systems (O. D. Harkelroad, R. D. Turner)

The work on the 3.25-MW ac-dc power system during 1978 was to rebuild the control system so that it could be manually operated with a water-cooled resistor as a load. Instrumentation and control circuits necessary to perform no-load, high-voltage tests were completed and checkout tests were begun.

*Factors are for freight cars; other values are substituted for passenger cars and locomotives.

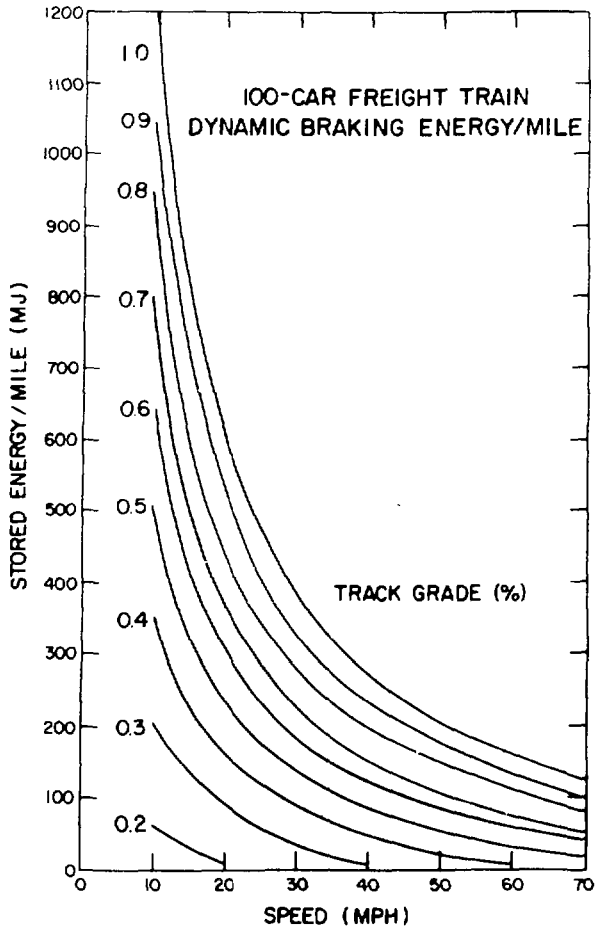

Fig. 14.
Available train energy for storage as a function of speed and percent grade.

Dielectric tests were run on oil samples taken from several locations in the induction voltage regulator (IVR) and the rectifier transformer. Results from two independent tests showed that the breakdown voltage of the oil samples was above 40 kV, which is above the specified limits. The high-voltage switchgear and the three-phase surge-current and over-current protection systems were checked.

The first attempt to energize the rectifier transformer at no load resulted in a line-to-ground fault in the IVR. This caused the surge-current relay protection system to deenergize the system. A post-fault inspection

showed no damage to the switch gear but the main winding of one of the IVRs duplex-triplex rotor units was severely damaged.

Based upon the disassembly inspection, the line-to-ground fault is believed to have been caused by an insulation degradation from moisture leakage through a broken high-voltage bushing. This bushing fracture was probably caused by busbar misalignment stress in reassembly, which followed the power supply's relocation. The IVR has been removed and sent to the General Electric Service Shop for repair. It will be returned for reinstallation in early 1979.

B. 7.5-kA Battery Power Supply (H. J. Boenig, M. J. Bowden, C. Quihuis, W. D. Smith, S. Rose)

The fabrication of a 7.5-kA, series-regulated, transistor power supply was completed. Six 2-V, 1200-Ah batteries are connected in parallel and form the power source. The series regulator consists of 40 water-cooled plates, each with twelve 60-A transistors.

A digital current controller for the 7-kA battery power supply is nearly completed. This system will allow constant current operation over a programmable range of 0 to 4000 A with 1-A resolution. The controller incorporates a high-speed analog-to-digital converter and display circuit for slewing rates of 10 kA/s without oscillation. Digital feedback provides a circuit which is almost entirely self-compensating with reduced low-frequency noise and drift problems.

C. DEC-PDP 11/34 Minicomputer Software (H. J. Boenig, S. Rose, R. D. Turner)

Several hardware and software additions were made to the minicomputer system to improve its overall performance and usage. An AD-11 kT data acquisition package and the associated software were purchased and installed. The package includes a 16-channel analog-to-digital converter, a programmable clock, and a 48-channel multiplexer, which results in providing 64 single-ended or 32 differential channels. A new, more powerful operating system (version 3B of RT-11) was installed. This resulted in reduced execution times and simplified program handling and editing. An FP-11A floating point processor was installed and made operational. With the FP unit, FORTRAN program execution times have been effectively cut in half. The copy of the RT-11

FORTRAN IV scientific subroutine package was purchased. The package, which includes routines for matrix operations and statistical and numerical computations, improves the usefulness of the computer for mathematical analysis.

D. Data Acquisition System (M. J. Bowden)

A general-purpose data acquisition and processing system that uses the PDP-11/34 minicomputer was developed. Software for this system consists of two major programs that operate independently through permanent data files. The first program performs the initialization, data acquisition control functions, permanent file management, and preprocessing. The initialization procedure defines the type and transfer rate of data to be recorded, as well as information necessary for subsequent processing, e.g., channel gain factors, data minimums and maximums, etc. These parameters are retained as defaults, allowing one-button data acquisition for tests in which the input assignments do not vary.

The programmable clock provides a wide range of sample speeds plus substantial high-frequency noise rejection. Noise levels are comparable to direct analog measurements, with the added convenience of digital filtering. The computer is capable of acquiring data on 1 to 64 analog input channels at a total throughput rate of over 20 000 samples per second. Uninterrupted storage capacity exceeds 1 million 12-bit data points.

The second program implements display terminal graphics and processing functions. Interactive graphics subprograms allow the operator to examine data from any set of input channels with automatic or user-selected scaling. Single key instructions display direct voltage and time measurements or operator-defined equations for signals representing other quantities. Equations may include arithmetic combinations of data channels and constants (vector operations) for conversion to actual data coordinates.

Performance of the data acquisition system is better than originally expected and will lead to large savings in experimental data analysis time as well as increases in accuracy. Both programs are now entirely operational.

The low signal levels and unusual grounding requirements in many experiments necessitate special signal conditioning amplifiers. Although additional amplifiers will be required for full use of the expanded capacity, this is the only hardware limitation in the present system.

IX. PUBLICATIONS AND PAPERS PRESENTED

Bennett, J. G., Anderson, C. A., "Structural Design for a 10-GWh SMES Vacuum Vessel," Los Alamos Scientific Laboratory report LA-7110-MS (January 1978).

Rogers, J. D., "Superconducting Magnetic Energy Storage (SMES) Program, January 1 - December 31, 1977," Los Alamos Scientific Laboratory report LA-7294-PR (August 1978).

Hassenzahl, W. V., Rogers, J. D., "Workshop on Stability in Superconducting Magnets, Los Alamos, New Mexico, July 25-29, 1977," Los Alamos Scientific Laboratory report LA-7297-C (June 1978).

Boenig, H. J., Bronson, J. C., Colyer, D. B., Hassenzahl, W. V., Rogers, J. D., Schermer, R. I., "A Proposed 30-MJ Superconducting Magnetic Energy Storage Unit for Stabilizing an Electric Transmission System," Los Alamos Scientific Laboratory report LA-7312-P (June 1978).

Migliori, A.M., Schermer, R. I., Henke, M. D.,"Dielectric Tracking in Liquid Helium," Cryogenics 18, 443 (1978).

Keller, W. E., "Low Temperature Physics and Engineering Quarterly Progress Report, January 1 - March 31, 1978," Los Alamos Scientific Laboratory report LA-7374-PR (July 1978).

Bennett, J. G., Anderson, C. A., "Structural Design for a 10-GWh SMES Vacuum Vessel," Joint ASME/CSME Pressure Vessels and Piping Conf., Montreal, Canada, June 25-30, 1978; paper 78-PVP-46.

Keller, W. E., "Low Temperature Physics and Engineering Quarterly Progress Report, April 1 - June 30, 1978," Los Alamos Scientific Laboratory report LA-7448-PR (September 1978).

Rogers, J. D., Boenig, H. J., Hassenzahl, W. V. , Schermer, R. I., "Superconducting Magnetic Energy Storage," presented to Institute of Gas Technology, Chicago, IL, July 10, 1978.

Schermer, R. I., "An Experimental and Theoretical Study of the Effect of Local Heating on Composite Superconductors," 1978 Applied Superconductivity Conference, Pittsburgh, PA, September 25-28, 1978.

Rogers, J. D., Boenig, H. J., Bronson, J. C., Colyer, D. B., Hassenzahl, W. V., Turner, R. D., Schermer, R.I., "30-MJ Superconducting Magnetic Energy Storage (SMES) Unit for Stabilizing an Electric Transmission System," Applied Superconductivity Conference, Pittsburgh, PA, September 25-28, 1978.

Rogers, J. D., Boenig, H. J., Hassenzahl, W. V., Schermer, R. I., "Superconducting Magnetic Energy Storage for Electric Utilities and Fusion Systems," Instrument Society of America 1978 National Conference and Exhibit, Philidelphia, PA, October 15-19, 1978.

Rogers, J. D., Boenig, H. J., "Superconducting Magnetic Energy Storage," Dept. of Energy Contractors' Meeting on Energy Storage, Luray, VA, October 24-26, 1978.

REFERENCES

1. J. G. Bennett and C. A. Anderson, "Structural Design for a 10-GWh SMES Vacuum Vessel," Transactions of the ASME, Journal of Pressure Vessel Technology 100, 263-270 (1978).

2. J. G. Bennett and C. A. Anderson, "Structural Design for a 10-GWh SMES Vacuum Vessel," Los Alamos Scientific Laboratory report LA-7110-MS (January 1978).

3. K. T. Hartwig, "Wisconsin Superconductive Energy Storage Project," Engineering Experiment Station, University of Wisconsin, Madison Report, EES report 47 (May 1977).

4. G. F. Fuh, T. Doe, and B. C. Haimson, "Design of Underground Tunnels for Superconductive Energy Storage," Supplemental Volume, Eighteenth US Symposium on Rock Mechanics, US National Comm. Rock Mech., National Acad. Sci., F. Wang, and G. Clark, Eds., (Colorado School of Mines Press, Boulder, CO, 5A5-1 to 5A5-6 (1977).

5. S. P. Clark Jr., "Handbook of Physical Constants," Geol. Soc. Am. Mem. 97, 587 pp., 1966.

☆ U.S. Government Printing Office: 1979 — 677-013/23